International Journal of Thermofluids 23 (2024) 100734

Contents lists available at ScienceDirect

International Journal of Thermofluids

journal homepage: www.sciencedirect.com/journal/international-journal-of-thermofluids

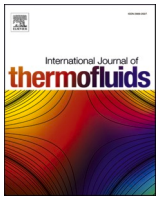

Unveiling the inherent properties and impact of ultrafine nanobubbles in polar and alcoholic media through unsupervised machine learning and atomic insight

Hamidreza Hassanloo *, Xinyan Wang

Centre for Advanced Powertrain and Fuels, Brunel University London, Uxbridge, UB8 3PH, United Kingdom

ARTICLE INFO

Keywords:
Bulk nanobubbles
Nucleation and Stability
Thermophysical properties
Unsupervised machine learning
Molecular dynamics simulation

ABSTRACT

The presence of dissolved gas in the host medium in various industrial processes, such as the presence of oxygen and hydrogen during water splitting or carbon dioxide in fuel cells, or the dissolution of nitrogen for industrial applications, increases the probability of the formation of bubbles at nano-scale. Nanobubbles (NBs), spanning tens to hundreds of nanometres, display exceptional attributes, including remarkable stability, enduring longevity, and an impressive surface-to-volume ratio. These qualities firmly position NBs as pivotal entities with applications that extend across diverse industries, encompassing fields such as energy and chemistry. Therefore, it is crucial to have a comprehensive understanding of their inherent properties and behaviour right from the nucleation stage to grasp their distinctive traits fully. This paper focuses on the combination of data-driven and molecular dynamics simulation to provide a clear understanding of the mechanisms behind NBs nucleation and behaviour in liquids and identify their characteristics. The nucleation process of four gases in two potential liquids for hosting NBs, namely water and methanol, was investigated through scattering nitrogen, oxygen, carbon dioxide, and hydrogen in host liquids using molecular dynamics simulations. Then, high-throughput screening based on the DBSCA (density-based spatial clustering of applications with noise) algorithm was used to screen the formed NB clusters through dissolved gases in the host liquids to determine the size of formed NBs, their density, and motion over time. The findings offer unique insights, indicating that the density of the surrounding liquids is altered and decreased by formed nanobubbles, influenced by the establishment of a nanolayer. The lowest density was recorded for hydrogen and nitrogen nanobubbled methanol samples at 0.61673 and 0.68918 g/ml, respectively, and for hydrogen and nitrogen nanobubbled water samples at 0.93797 and 0.93722 g/ml, respectively. Additionally, the highest density among the scattered gases was observed in non-nanobubbled carbon dioxide methanol and water samples at 0.77724 and 0.99588 g/ml, respectively. Furthermore, the viscosity of the host liquids is influenced, particularly in the presence of high-density nanobubbles, as the highest viscosity was observed for nitrogen nanobubbled water samples at 0.00103 Pa.s.

Introduction

The increasing global demand for efficient heat transmission systems, driven by the need to reduce thermal losses, optimize system costs, enhance heat removal and transportation, and prolong the lifespan of utility systems, underscores the critical role of thermophysical properties of working fluids [1]. These properties govern essential parameters such as the heat transfer coefficient, pressure drop, and energy efficiency, constituting fundamental metrics for assessing the performance of thermal systems [2]. Consequently, significant efforts have been directed towards replacing traditional thermal fluids with those possessing improved thermophysical characteristics. Notably, nanoscale phenomena have a significant impact on these attributes, as nanoparticles or nanoscale mechanisms govern fluid properties such as viscosity, density, and rheological behaviour [3,4]. This influence could be amplified when dissolved gases are introduced into working fluids, particularly in industrial processes like electrochemical reactions used in energy conversion and storage, where gaseous byproducts like hydrogen and oxygen often emerge, potentially leading to alterations in the thermophysical properties of the host liquid [5-7]. This alteration becomes even more pronounced when these gases tend to give rise to nanobubbles (NBs) [8].

* Corresponding author
E-mail address: Hamidreza.Hassanloo@brunel.ac.uk (H. Hassanloo).

https://doi.org/10.1016/j.ijft.2024.100734

Available online 13 June 2024

NBs, which are defined as gaseous cavities with diameters smaller than 1 μm, can be classified into two main categories: surface NBs and bulk NBs. Surface NBs typically exhibit heights ranging from greater than 10 nm to less than 100 nm, along with contact line pinning from 50 to 500 nm. In contrast, "bulk NBs," also known as "ultrafine bubbles," are generally spherical, gas-filled structures with diameters less than 1000 nm exhibit unique properties, such as enduring longevity, and an impressive surface-to-volume ratio, that make them to become versatile sensing materials with applications spanning diverse industrial and chemical processes [9,10], encompassing electrochemical reactions [7, 11], as well as practical uses like water purification [12,13], promoting the growth of animals and plants [14], ensuring surface sanitation [15], drug delivery [16], and powering energy-related applications [17,18].

Exploring these minuscule bubbles through experimental techniques [19-21] presents formidable challenges, as some methods struggle to distinguish NBs from other nanoscale contaminants, and the fundamental processes governing NB behaviour and inherent properties remain elusive [22,23]. One of the most intriguing and extraordinary aspects of these tiny bubbles is their exceptional stability, defying the predictions of the Epstein-Plesset theory, enabling them to persist in host liquids for extended periods and significantly influencing practical applications [24,25]. Their divergence from conventional continuum theories adds further complexity to the investigation of NBs. This complexity is accentuated when dealing with bulk NBs, which, unlike surface-bound NBs, are influenced by Brownian motion [26-28]. In tandem with experimental techniques, molecular approaches such as molecular dynamics (MD) simulations offer a means to attain a molecular-level understanding of the characteristics, behaviours, and impact of these nanoscopic bubbles.

Ohgaki et al. [29] prepared enriched distilled water with methane, nitrogen, and argon by using rotary pump under the atmospheric conditions at 298 K. Replica film for scanning electron microscopic observation was utilized to measure the size of NBs and it was revealed by Raman spectroscopy that the huge amount of dissolved nitrogen molecules existed in the form of NBs and there is few nitrogen molecules scattering homogenously in the surrounded medium. The lifetime of the observed NBs was estimated to be more than two weeks due to the strong hydrogen bond on the interface that avoid the penetration of gas molecules from NBs. Diffusive shielding was suggested as a stability mechanism for bulk NB clusters by Weijs et al [30]. In a numerical study they implemented quasi-2D molecular dynamics simulation of Lennard-Jones (LJ) binary liquid to scrutinize this notion. Two initial configurations were prepared. One of them included a pre-existed bulk NB while the gas molecules were scattered in the other one. They reported that nucleation happened for a high concentration of dispersed gas. In addition, they declared that NBs should be close together in order to keep the medium around each other saturated before the NBs disappear entirely. In another investigation, a molecular approach was employed to investigate the nucleation and agglomeration of methane NBs during the gas hydrate dissociation process [31]. It was demonstrated that specific conditions, such as the concentration of diffused gas molecules, triggered the formation of NBs from the released CH_4 molecules. In addition, the majority of the dissolved gas underwent NB formation. The notion of using hydrogen nanobubbles (HNBs) for conversion from traditional energy-based economy to hydrogen economy was investigated in an experimental study [32]. As current technologies for hydrogen storage are not proper for practical applications, researchers have tried to use high stability of HNBs to store them in a quasi-2D system include Keyhole limpet hemocyanin and organic molecules. An electron radiolysis assisted abstraction reaction was used to generate HNBs. It was observed that beyond specific concentration the nucleation and growth of HNBs would continue and designed system could meet the target of hydrogen storage set out by Department of Energy (DOE). Bhushan et al. [33] conducted an experimental study to investigate the motional behaviour of formed NBs in deionized water with polystyrene (PS) coated silicon wafer as a substrate by using atomic force microscopy (AFM) in the tapping mode (TMAFM). It was revealed that NBs are very sensitive to scan parameters. In addition, they observed that the velocity of the movement of smaller NBs was higher than that of bigger ones and the tiny NBs tended to merge and coalescence to form bigger NBs. In a numerical study, Koishi et al [34] investigated the formation of NBs by using molecular dynamics simulation and applied simple point charge/extended (SPC/E) and optimized potentials for liquid simulations (OPLS) potentials to simulate the interaction between water and CH_3 units, respectively. They defined two polar and non-polar zones. Polar zone consisted of water molecules, with fixed centre of mass and freedom in rotation, while non-polar zone was constructed with CH_3 units. The cavitation, which was consider as a NB, was observed when the distance between CH_3 units was small. By increasing the distance of the units, the probability of NBs formation decreased. In general, NBs are a relatively new research area, with most studies emphasizing the stability of pre-defined NBs in host liquids. In a study by Zhang et al. [35] the impact of nitrogen molecules on the stability of nitrogen NBs in water was investigated, revealing a strong correlation between nitrogen gas concentration and NB stability. Furthermore, the stability of different-sized oxygen NBs in water was assessed, with an important role identified for supersaturation in NB stability, especially for smaller NBs [36].

Previous research has been crucial in advancing our understanding of NBs, particularly in their formation, stability, and applications. This involves exploring gas concentration's role in NB formation [31], the effects of diffusive shielding [30] and dynamic behaviours [33] on NBs stability. Moreover, this research has unveiled potential applications for NBs [32].However, it's essential to note that most studies have been limited in scope, focusing primarily on surface NBs and pre-defined bulk NBs [37-40]. For instance, the enhancement in the etching process of gold nanorods was reported in the presents of pre-defined oxygen NB. [41]. However, the behaviors and mechanisms governing bulk NBs, particularly during their nucleation stage, which holds paramount importance in industrial applications [42], have been left relatively unexplored. Moreover, these studies have primarily focused on the fundamental aspects of NBs, overlooking their engineering applications. Even in the realm of fundamental research, which has been explored through molecular approaches to gain insights into NB behaviour and characteristics, challenges persist. Researchers face not only the computational demands imposed by large simulation boxes in molecular dynamics simulations but also the formidable task of handling and processing the substantial volumes of data generated by these simulations. To overcome this challenge, researchers may resort to certain assumptions, such as fixing the centre of pre-defined NBs, to facilitate more detailed investigations into NB behaviour [36]. However, such assumptions may compromise the accuracy of analyses concerning the motion and dynamics of NBs, potentially failing to capture their real-world behaviour accurately. Machine learning (ML) plays a crucial role in handling vast datasets generated by atomistic and molecular simulations across various scientific domains, such as material science, solid-state physics, biophysics, and biochemistry. Machine learning encompasses three primary categories. Supervised learning relies on input-output pairs for predictions, commonly used in material and molecular property forecasting. In reinforcement learning, models learn through continuous interaction with their environment, without initial data. Unsupervised learning primarily focuses on extracting valuable insights solely from input data, commonly applied in molecular simulations to generate compact descriptors, including clustering and low-dimensional collective methods, for analysing molecular trajectories [43].

A more systematic and data-driven approach, involving the nucleation of various NBs in diverse liquid hosts, holds the potential to yield profound insights into the characteristics and mechanisms governing the nucleation and subsequent behaviour of bulk NBs and their impact on the inherent properties of host liquids. In this study, a hybrid methodology is employed, combining molecular dynamics simulations with

unsupervised machine learning technique, to evaluate the probability of NB formation resulting from the dissolution of nitrogen, oxygen, carbon dioxide, and hydrogen— each extensively utilized in chemical processes and industrial applications such as water splitting [44] and enhanced oil recovery [45]. Additionally, this research delves into the intrinsic characteristics of formed nanobubbles (NBs) and their influence on the thermophysical properties of host liquids, crucial in fluid applications. Exploring these inherent heat transfer fluid properties encompasses the examination of density and viscosity. Density significantly shapes fluid flow and heat transfer, impacting Reynolds number, Nusselt number, friction coefficient, and pressure loss. Temperature-induced density shifts can drive natural convection [46]. Viscosity, another critical property, profoundly affects various energy-related applications like heat transfer systems and pumping processes. Higher viscosity escalates frictional losses, reducing overall energy transfer efficiency and requiring more pumping energy. Conversely, lower viscosity enhances flow dynamics, lowering energy consumption. Employing the Green-Kubo method, this study calculates the viscosity of water and methanol-based samples, serving as a vital bridge between fundamental principles and their practical engineering applications. The investigation encompasses two host liquids, water and methanol, both of considerable industrial importance. Water holds a pivotal position across a wide range of industrial applications, particularly in renewable energy applications [47]. Additionally, methanol serves as a valuable renewable energy carrier and holds a critical role as a renewable fuel alternative, known for its substantial hydrogen storage capacity [48,49]. Commencing with a discussion of theory and modelling setups, this paper will subsequently delve into an in-depth analysis of NBs characteristics and their influence on thermophysical properties in the Results and Discussions section.

Theory and modelling

The evolution of science can be understood through four major paradigm shifts. Initially, empirical studies were conducted, followed by the collection and sharing of research, which provided a more comprehensive perspective on scientific issues and led to the development of key theoretical foundations. With the development of computational systems, complex calculations become more feasible, leading to a deeper understanding of scientific phenomena through technology-driven advancements in scale. The most recent shift is the emergence of the Fourth Paradigm, which is dominated by big-data-driven science, characterized by an overwhelming influx of data and associated systems and analytics to process it [50].

Computational nanoscience investigates the behaviour of molecules and interactions between atoms. Essentially, computational nanoscience is a powerful tool that enables the investigation and comprehension of the mechanisms governing nanoscale phenomena at the molecular level. This modern science gives a unique opportunity to researcher to appraise their new notions by observing and manipulating the behaviours of next generation materials [51,52]. Molecular dynamics simulations use Newton's second law to predict the motion of atoms by using various potentials as a foundation stone to calculate the exerted force on each atom [53]. In this study an all-atom optimized potentials for liquid simulations (OPLS) force field, TIP4P/2005, transferable intermolecular potential with 4 points, model and Lenard-Jones potential have been applied to simulate the interaction of atoms of methanol, water, and gases. OPLS is inherently united-atom force field. Generally, the computational cost of fluids simulation depends on the number of interaction sites squared. In united-atom approach, non-bonded interaction sites are considered on non-hydrogen atoms and hydrogen atoms that attached to carbons in aromatic rings. Increasing the interaction sites in all-atom method improves the accuracy of charge distribution and torsional energy that brings about the improvement in capturing the interaction of molecules. The bond stretching and angle bending parameters of all-atom approach were adopted from assisted model building with energy refinement (AMBER) all-atom force field, while the torsional parameters were calculated from the ab initio molecular orbital calculation [54-59].

All the simulations were carried out by the open source LAMMPS [60], large-scale atomic/molecular massively parallel simulator. Ovito software [61] was used as the visualization tool. In the first place, inherent properties of methanol and water were calculated with the selected potentials. Table 1 shows the calculated thermophysical properties of methanol and water and the reported experimental values. Comprehensive details of the simulation procedure are available in the supplementary file.

Then, the effect of dissolved gases, host liquids and operation temperature on the formation, growth, and characteristic of NBs were investigated. In the initial phase, all samples underwent a 1.7 ns equilibration period in both NPT, constant number of particles, pressure, and temperature, and NVT, constant number of particles, volume, and temperature, ensembles, followed by a 10 ns evolution in the NVE, constant number of particles, volume, and energy, ensemble. Utilizing a molecular approach, the study delved into the exploration of thermophysical properties and the tracking of atomic motion over time. The temporal and spatial data collected from molecular dynamics simulations were subsequently utilized in a high-throughput screening process to identify clusters of NBs formed through the scattered gases within the host liquids. This screening involved an assessment of the gas atom count within these clusters, as well as their density, radius, and motion over time. As shown in Fig. 1, this study combines elements from the last two scientific inquiry paradigms. Machine learning is commonly employed for tasks such as classifying data into distinct categories (classification) or forecasting numerical values (regression). Classification entails assigning labels or categories to input data by discerning patterns within the dataset, while regression involves predicting continuous numerical values based on input features. ML techniques are applicable for categorizing or analyzing extensive datasets derived from molecular dynamics simulations, including those spanning long simulation durations and featuring numerous atoms.

Clustering, an unsupervised machine learning technique, is employed to divide a set of particles into meaningful subgroups (clusters) by minimizing similarities between clusters and maximizing within-cluster similarities. DBSCAN (density-based spatial clustering of applications with noise), a well-established density-based clustering algorithm known for its ability to identify clusters, is utilized [64]. Derived from MD simulations, the dataset, including particle positions within the system, serves as input for an in-house code developed using this efficient algorithm, facilitating the analysis of NB characteristics via trajectory data and offering insights into the influence of molecular interactions on their behaviour.

Results and Discussion

Characteristics of nanobubbles

Methanol and water were used as solvents to dissolve nitrogen, oxygen, carbon dioxide, and hydrogen gases. Samples with a 6%-weight fraction of dissolved gases were prepared by scattering 2422, 2120, and 1542 nitrogen, oxygen, and carbon dioxide molecules, respectively, in

Table 1
Inherent properties of methanol and water under the environmental condition [62,63].

Liquids	Number of atoms	Potential	Density (g/ml)	Viscosity (Pa.s)	Diffusion Coefficient (m^2/s)
Methanol	156000	OPLS	0.77	0.00052	$2.52x10^{-9}$
		Experimental	0.79	0.00053	$2.44x10^{-9}$
Water	177000	TIP4P/2005	0.98	0.000096	$2.30x10^{-9}$
		Experimental	0.99	0.000089	$2.30x10^{-9}$

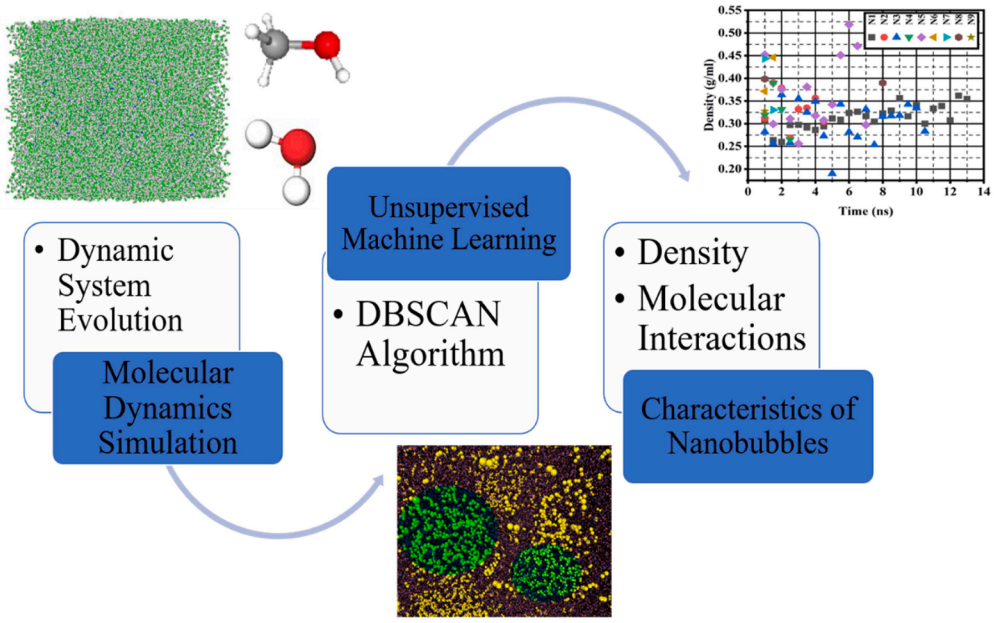

Fig. 1. Methodological framework for studying nanobubbles, involving temporal atom coordinate extraction through molecular dynamics simulation, unsupervised machine learning for nanobubble detection, comprehensive characterization of nanobubbles, and elucidation of underlying behavioural mechanisms.

59000 water molecules. To achieve the same gas concentration in methanol, 1899 nitrogen, 1662 oxygen, and 2231 carbon dioxide molecules were dispersed in 26000, 26000, and 48000 methanol molecules, respectively. Due to its small mass fraction, different concentrations of hydrogen gas were used. Samples containing 59000 water molecules and 26000 methanol molecules housed 2422 and 1905 hydrogen molecules, respectively, scattered within them. The initial configuration of the prepared samples is presented in Fig. 2. Investigating such samples, which encompass a substantial number of molecules and evolve over more than 13 nanoseconds, leading to the formation, coalescence, and interaction of NBs with surrounding molecules, generates vast datasets. These datasets pose challenges when examining parameters such as density, gas molecule quantification within NBs and the surrounding liquid, and size. To investigate these intricate dynamics comprehensively over time, the utilization of both molecular dynamics simulation and unsupervised machine learning proves instrumental in studying the ultrafine bubbles in more detail.

It was observed at 298.15 K and 1 atm that nitrogen, oxygen, and hydrogen can form NBs in water. The formation of NBs begins with the emergence of nucleation sites within the host liquid. Fig. 3 visually depicts the formation of NBs within the host liquids at 1 ns. Furthermore, it illustrates the temporal evolution of the number of bulk NBs formed in the host liquid over time. It is clear that for the same weight fraction of the dissolved gases the number of nucleation sites highly depends on the type of the scattered gas. Nine nitrogen NBs were formed initially while only 2 oxygen NBs were formed in water at 1 ns. The nucleation process in hydrogen/water sample is driven by 1 nucleation site.

In contrast to the water host liquid, oxygen does not exhibit the formation of NBs in methanol. Notably, the nucleation of nitrogen NBs commenced with the presence of 2 NBs in methanol at 1 ns. This observation underscores the significant influence of the host liquid on the nucleation of NBs (Fig. 4).

Water molecules have a stronger attraction to each other than methanol molecules due to their ability to form hydrogen bonds [65]. In the case of water, the limited availability of interaction sites between dissolved gas molecules and water molecules results in a more substantial attractive force among nitrogen molecules, as depicted in Fig. 5. Consequently, the nucleation of nitrogen within a water host liquid occurs with a higher number of nucleation sites. Conversely, in methanol, the weaker interactive forces between methanol molecules enable them to have stronger attractive forces with dissolved oxygen gas. This

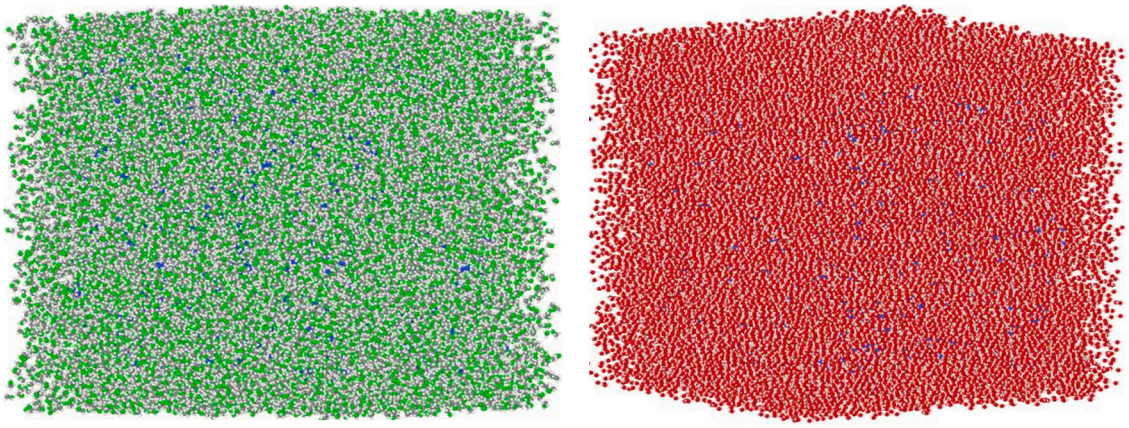

Fig. 2. Initial structure of the dispersed gas in methanol (left) and water (right).

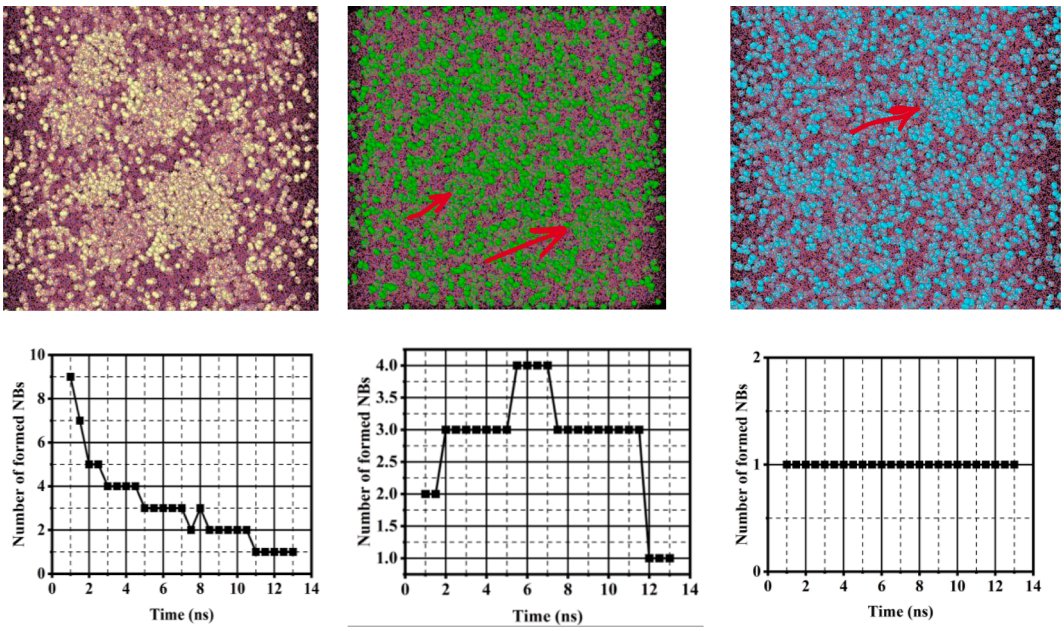

Fig. 3. Snapshots at 1 ns (top) and evolution of the number of formed (bottom) nitrogen (left), oxygen (centre), and hydrogen (right) NBs in water over time.

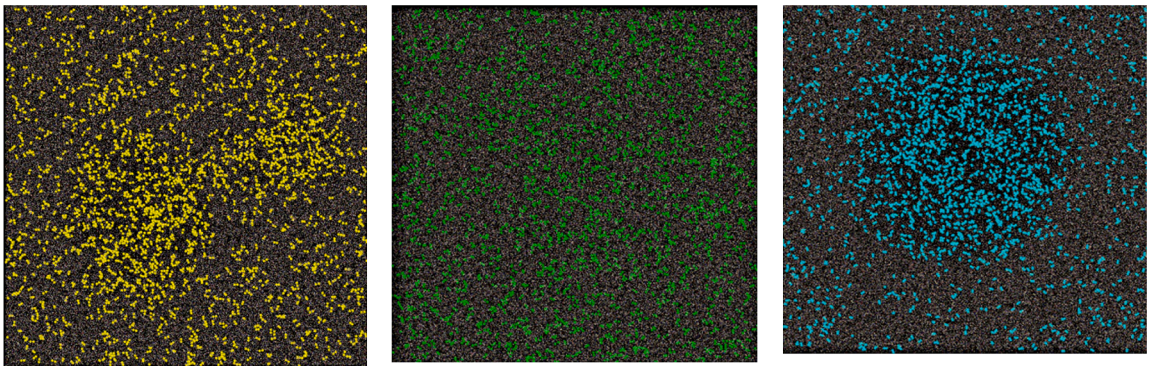

Fig. 4. Snapshot of formed nitrogen (left), oxygen (centre) and hydrogen (right) NBs in methanol at 1 ns.

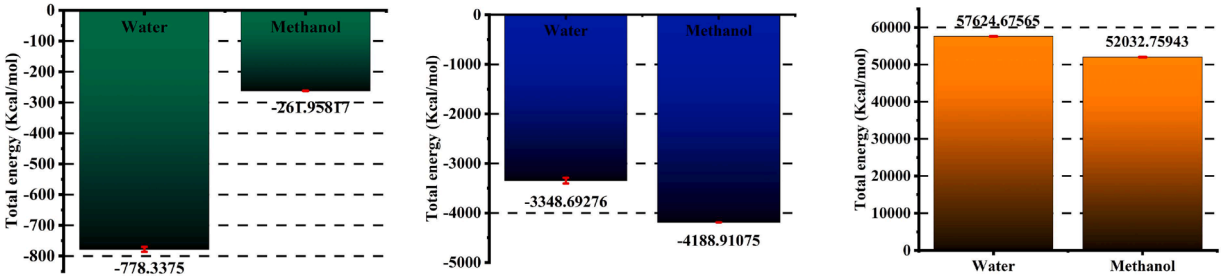

Fig. 5. The average of total energy between nitrogen-nitrogen (left) oxygen-host liquid (centre) and carbon dioxide- carbon dioxide molecules (right) in water and methanol.

strong attraction prevents oxygen gas from coming together to form NBs in a methanol host liquid, in contrast to water. Furthermore, it's worth noting that carbon dioxide is unable to form NBs in both water and methanol. This is illustrated in Fig. 5, where a substantial repulsive force between carbon dioxide molecules prevents their aggregation within the host liquids. This repulsive force arises from the electron distribution around the oxygen and carbon atoms, resulting in partial positive charges on carbon atoms and partial negative charges on oxygen atoms. These opposing charges lead to a net repulsive force between carbon dioxide molecules. Moreover, it is interesting that the majority of the dissolved nitrogen gas exist in the form of NB, only 27.41% of dispersed nitrogen gas remains scattered, after 13 ns in water. However, 27.27% and 34.11% of dissolved oxygen and hydrogen gas exist in the form of NB in the polar host (Supplementary Fig. 4). Therefore, the nucleation morphology and formation of NBs are affected by the solubility of the dissolved gas. Although the solubility of hydrogen is less than oxygen [66], only one nucleation site was observed in hydrogen/water sample. The intermolecular interaction between gas atoms reveals that attractive

force between gas molecules is another factor that affects the morphology of nucleation of NBs. The attractive forces between non polar molecules are primarily due to London dispersion forces which originate from the temporary distortion of electronic distribution within molecules, facilitated by the dynamic nature of electron motion. The London dispersion forces result in a transient nonzero dipole moment for the molecule and induce similar dipoles in neighboring molecules, leading to attractive forces between them. The magnitude of these dispersion forces depends on the polarizability of the molecules. Valence electrons in heavier and larger atoms or molecules are more distant from the nuclei than that in smaller atoms or molecules, resulting in weaker electron-nucleus attractions. This makes them more susceptible to forming temporary dipoles [65,67]. Therefore, attraction force in oxygen atoms is larger than the hydrogen atoms, oxygen atoms tend to agglomerate in water host faster than hydrogen atoms and lead to several nucleation sites.

The density of the formed NBs over time was calculated using unsupervised machine learning, as depicted in Fig. 6, more detail has been provided in Supplementary File. Notably, the density of these generated NBs is significantly greater than the density of the gas present in the gas phase. Upon comparing the density of the formed NBs with their respective sizes, as shown in Fig. 6, an intriguing pattern emerges. It becomes evident that the density of NBs increases as their size decreases. For instance, consider the case of nitrogen NB N5, which exhibits its highest density at 6 ns when it boasts its smallest size. Similarly, oxygen NB N3 showcases its peak density at 2 ns, coinciding with its smallest radius. The key here lies in the fact that smaller NBs possess a more substantial surface area-to-volume ratio compared to their larger counterparts. This increased surface area allows for heightened interaction with the surrounding liquid, resulting in stronger intermolecular forces between the gas and liquid phases. These intermolecular forces act to draw the gas molecules closer to the NB's surface, compressing the gas phase and resulting in a higher density when compared to larger bubbles. The attractive forces between gas and liquid molecules effectively create a compressive force that brings the gas molecules closer together. In the case of hydrogen NBs, it was observed that the highest density occurred at 7 ns, coinciding with the smallest size of the formed hydrogen NB at 1 ns. This behavior can be attributed to London dispersion forces, also known as London forces [66], which significantly affect the density of the formed NBs. As previously mentioned, it's important to note that attractive forces between hydrogen atoms are significantly weaker. As a result, when hydrogen gas atoms diffuse into the NB, they don't come closer together in the same manner as nitrogen and oxygen atoms. Consequently, hydrogen NBs do not exhibit the same trend of increasing density as their size decreases, in contrast to nitrogen and oxygen NBs. The density of NBs is a key factor contributing to their high stability within the host liquid [27]. It's worth noting that reducing the size of the formed NBs increases the attractive forces on their surfaces. This enhanced intermolecular interaction encourages gas atoms to absorb onto the NB, increasing its size while reducing its density. Therefore, this intermolecular interaction is pivotal in ensuring the stability of NBs within the host medium. To maintain NB stability, a sufficient concentration of scattered gas molecules must be present in the samples. In the interaction between gas atoms and formed NBs, attractive forces act upon both the NB and gas atom. Given that gas atoms are lighter than bulk NBs, gas atoms draw closer and are absorbed by the NB. This same mechanism can be extended to two bulk NBs. In this scenario, the NBs exert attractive forces on each other, causing the smaller NB to move more rapidly and approach the larger NB. Subsequently, as illustrated in Supplementary Fig. 5, the nearest gas atoms are initially absorbed and subsequently fully merge into the larger NB. In nanoscale systems, particle coarsening is governed by two primary pathways: Ostwald ripening and Smoluchowski ripening. Ostwald ripening involves larger particle growth and smaller particle reduction. Gas molecules detach from smaller particles and diffuse through the continuous phase, joining larger nanoparticles. Conversely, Smoluchowski ripening results from collisions among nanoparticles in motion through the continuous phase. Brownian motion induces random movements of NBs suspended in host liquid, causing collisions and subsequent coalescence. As a result, this process enlarges the average diameter of NBs while reducing their overall count [68]. During the coalescence process, atoms within the smaller NB deform it and establish a "bridge" with the larger NB, driven by London dispersion forces. As it is discussed, the attractive interaction leads to the movement of the

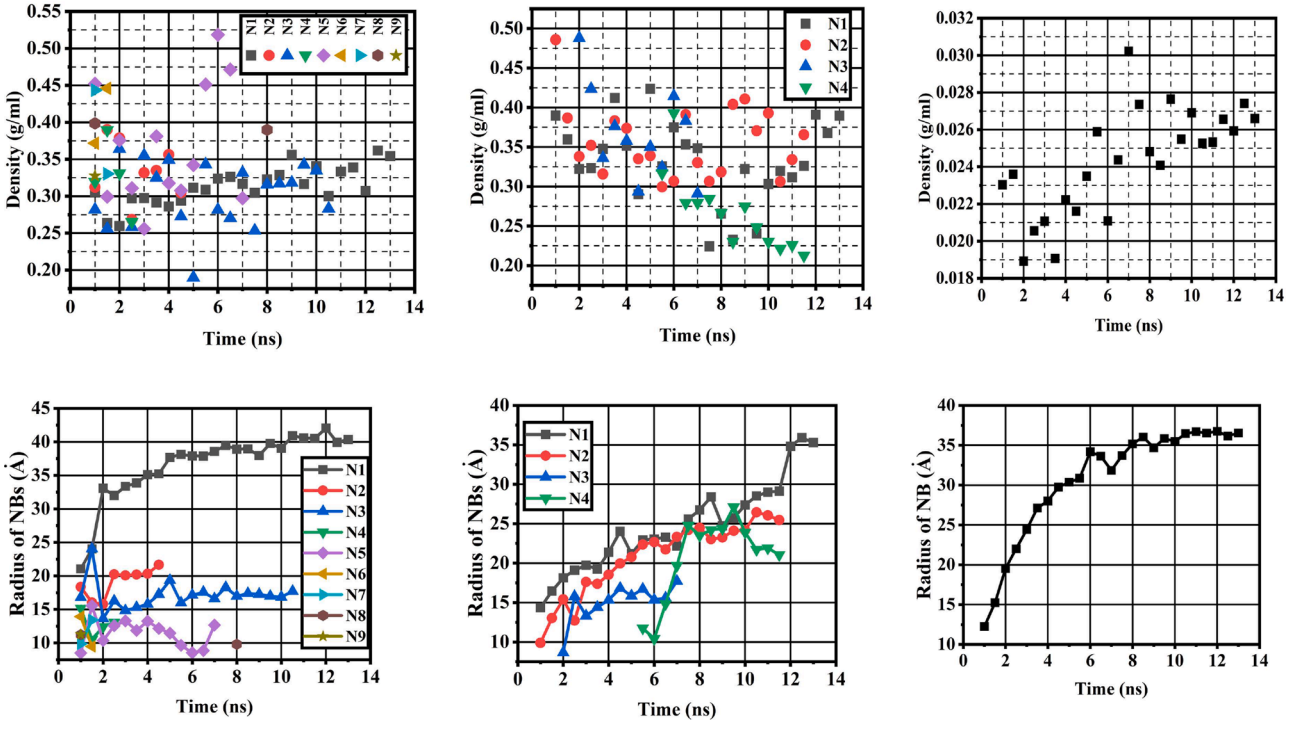

Fig. 6. Density (top) and the radius of formed (bottom) nitrogen (left), oxygen (centre), and hydrogen (right) NBs in water.

formed NBs within the prepared samples. Brownian motion also plays a role in increasing the stability of NBs. This motion arises from the random interactions of molecules in the surrounding medium. In contrast to macro and microscale bubbles, where buoyant forces act to push them upward due to density differences, Brownian motion introduces random molecular collisions that can move formed NBs in various directions, including downwards. This random movement can be sufficiently robust to counteract the buoyant force acting on NBs, effectively keeping them suspended within the liquid medium. The movement of average centre of final formed NB in water host liquid over time is depicted in Supplementary Fig. 6.

The final radius and density of the formed nitrogen and hydrogen NBs in methanol sample have been shown in Table 2. The comparison of obtained results for the formed NB in methanol (Table 2) and water (Fig. 5 and 10) reveal that the formed NBs in methanol host have bigger size and lower density than those generated in water. The density and size of formed NB can be affected the molecular interactions within the host liquids, which, in turn, govern the viscosity of the liquid. Diffusion of dissolved gases in more viscous solvent is less than low-viscosity one. Therefore, in less viscous host liquids like methanol more gas atoms can diffuse into a formed NB and produce larger NB in methanol compared to that in water. In addition, in a more viscous solvent, as it is difficult for the dissolved gas to move in host liquid, the trapped gas in NBs tend to have stronger interactions with each other, resulting in compact and denser NB. However, in less viscous liquid host, the trapped gas molecules have more freedom to move around and be further apart from each other, resulting in weaker attractive forces and less dense NB.

Temperature plays a pivotal role in shaping the formation and stability of nanobubbles within a host fluid. It exerts its influence by impacting various factors: firstly, the solubility of gases in the fluid is significantly affected by temperature, which subsequently shapes the behavior of nanobubbles. Secondly, temperature exerts control over the intermolecular forces and molecular interactions occurring within the liquid, consequently modulating the formation and properties of NBs. Notably, the dissolution of nitrogen gas in the host liquids has exhibited intriguing behavior, particularly in the formation of NBs at room temperature. This intriguing phenomenon has spurred further investigation into the influence of temperature on the nucleation and characteristics of nitrogen NBs in both water and methanol. To unravel these complexities, an investigation was conducted using dispersed nitrogen gas in polar and alcoholic host liquids at equal weight fractions, with examinations carried out at elevated temperatures of 343.15 K and 323.15 K for water and methanol, respectively.

Fig. 7 illustrates the number, radius, number of gas atoms and density of formed NBs in water host liquid at 343.15 K. Upon comparing Fig. 7 to Fig.s 3, and Supplementary Fig. 7, it becomes apparent that at higher temperature, nucleation is initiated by a smaller number of nucleation sites, which contain a higher concentration of gas atoms. As it was discussed, at room temperature nucleation is driven by 9 nucleation sites that the biggest one contains 515 gas atoms in the NB with 21.06 $\dot{A}$ radius. While at higher temperature, nucleation starts with 4 clusters and the biggest one is made up by 3007 gas atoms inside the NB with 49.18 $\dot{A}$ radius. It means that at higher temperature gas atoms have a greater tendency to be present in the form of NBs in the host liquid. In addition, it can be seen that the coalescence process in the sample at elevated temperature finishes sooner. At higher temperatures, the viscosity of the fluid decreases, making it easier for NBs to move and coalesce.

Table 2
Radius and density of the final formed NBs in methanol sample.

	Nitrogen	Hydrogen
Radius ($\dot{A}$)	48.510389	55.01482
Density (g/ml)	0.124979	0.007203

Fig. 8 illustrates the average of total energy between gas and liquid host atoms at two different temperatures. As it can be seen, by increasing temperature, the attractive force between gas and host liquid molecules reduces, which rise the tendency of scattered gas to agglomerate in the host liquid and form NBs. Furthermore, by comparing the density of NBs formed at higher and lower temperatures, it becomes apparent that increasing the temperature results in a decrease in the density of the formed NBs. Fig. 8 demonstrates that the increase in temperature results in a decrease in the attractive force between gas atoms, leading to a decrease in density.

Density and radius of the formed NBs in alcoholic sample at 323.15 K were measured at 0.081 g/ml and 53.30 $\dot{A}$, respectively. By comparing the obtained results with Table 2, it is clear that like water sample, properties of the formed NB are affected by temperature in the alcoholic sample, too. Furthermore, the dynamic of the formed NB in methanol host is also affected by temperature. Supplementary Fig. 8 showcases a sequence of snapshots at intervals of 0.5 ns, depicting the behaviour of the movement of average centre of final formed nitrogen NB in methanol sample at 298.15 and 323.15 K during the last 2.5 ns. It is evident that the formed NBs in methanol tend to rise to the surface at higher temperature, leading to reduction in the stability of the formed NB. As previously discussed, intermolecular forces, a significant factor influencing Brownian motion, contribute to the motion of molecules and formed NBs. Additionally, NBs suspended within a liquid encounter forces like drag force, which arises due to viscosity. Viscosity characterizes a fluid's resistance to flow, where higher viscosity leads to increased drag force acting on a suspended object. When the fluid's viscosity rises, the drag force on a NB intensifies, impeding its movement. Conversely, an elevated fluid temperature leads to decreased viscosity, reducing the drag force exerted on a suspended NB. Furthermore, a reduction in the NB's density amplifies the magnitude of the drag force. In the methanol sample, owing to its lower viscosity compared to water, temperature changes exert a greater influence on the balance of forces acting on the NB. This leads to a considerable reduction in the resistance force, causing the NB to rise. In summary, the dynamics and stability of formed NBs depend on the inherent properties of host liquids, particularly at elevated temperatures, with the resistive forces being pivotal factors.

Thermophysical Properties

Gas molecules, upon dissolving in a liquid, occupy the interstitial spaces between the liquid molecules, thereby expanding the solution's overall volume. This presence also disrupts the interactions among the liquid molecules, contributing to a subsequent decrease in density. Illustrated in Fig. 9 are the density alterations observed in the prepared samples, depicting a decline in the host liquid's density following gas dissolution. Furthermore, the emergence of nanobubbles in the sample intensifies this density decrease, notably showcasing that hydrogen nanobubbles exhibit the lowest density among the prepared samples.

When a NB nucleates in host solvent, gas molecules can form weak attractive interactions with the host medium molecules at the surface of the NB, which can cause the surface of the bubble to be coated with a layer of host liquid molecules. This means that the base fluid molecules in the nanolayer around the NB take up more space than if they were randomly distributed in the solution. In other words, the nanolayer contributes to a larger volume and lower density of the solution. Therefore, the interfacial layer between the NB and base fluid contains a smaller number of host liquid molecules. Fig. 10 shows the change of host liquid molecules near the NBs for various NB formed in the polar and alcoholic samples. It can be observed that the interfacial layer has a lower concentration of solvent molecules compared to the bulk liquid, and as the distance from the NB increases, the concentration of solvent molecules increases that can be concluded the presence of this layer disrupts the organization of molecules and results in a decrease in

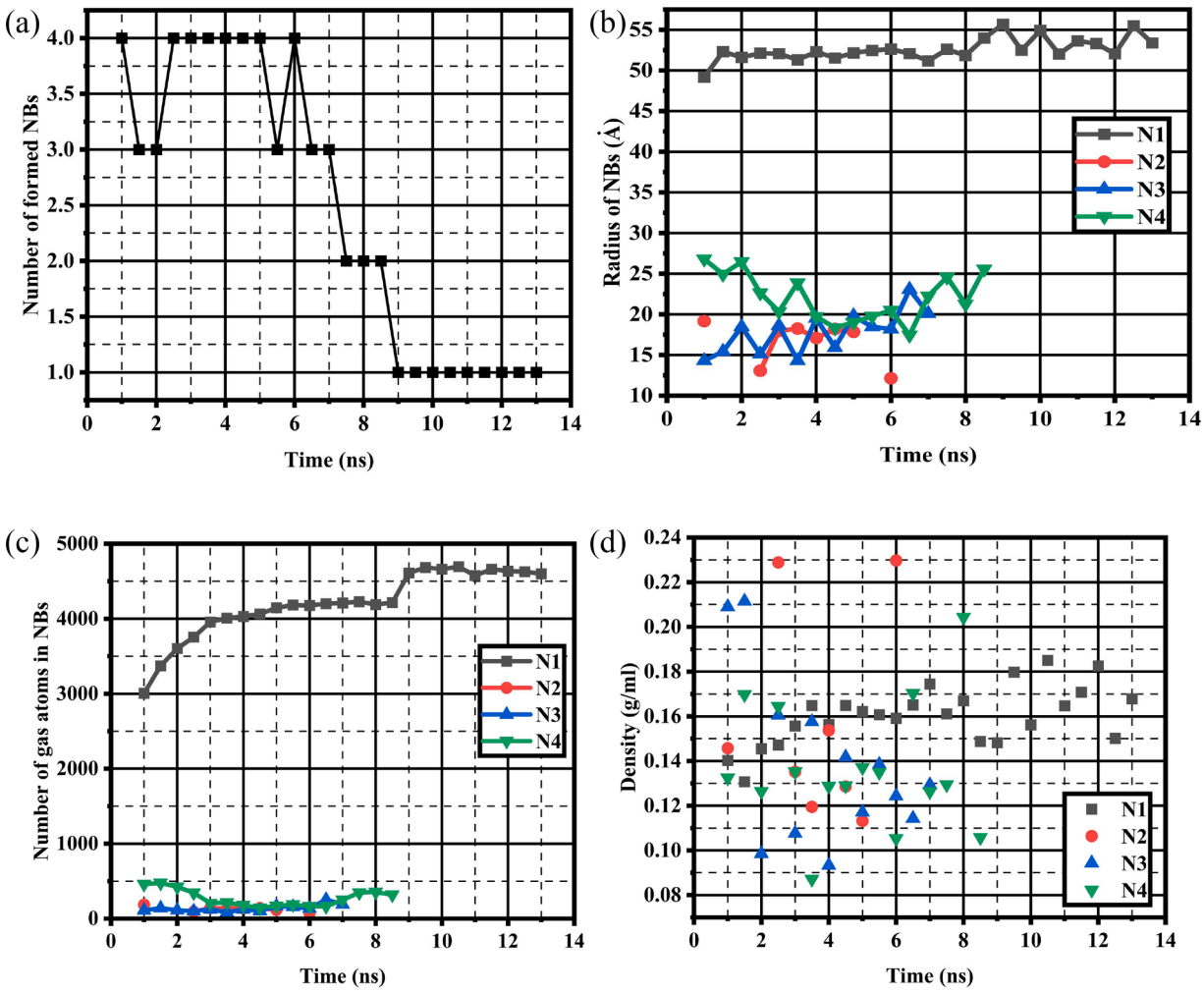

Fig. 7. (a) Number of formed nitrogen NBs, (b) radius of the NBs, (c) number of gas atoms inside the formed NBs, and (d) density of the nitrogen NBs at 343.15 K in water host.

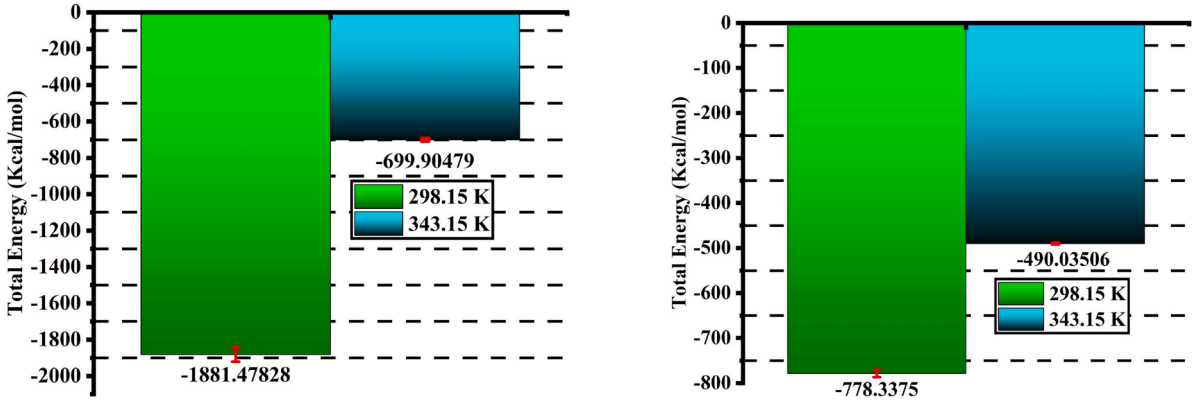

Fig. 8. The average of total energy between nitrogen gas and water (left) and between nitrogen gas atoms (right) in two different temperatures.

density.

In Fig. 11, the viscosity of samples containing dissolved gases in both water and methanol is depicted. The results reveal a notable contrast between the two host liquids. In the case of water-based samples, the inclusion of dissolved gases, including oxygen, nitrogen, carbon dioxide, and hydrogen, leads to an increase in viscosity compared to the pure host liquid. This trend aligns with previous research demonstrating that the viscosity of water tends to rise with gas dissolution [6]. Conversely, for methanol-based sample, a distinct behaviour is observed. Dissolution of nitrogen, hydrogen, oxygen, and carbon dioxide in methanol results in a reduction in viscosity compared to pure methanol [69]. This disparity in behavior between water and methanol highlights the significant influence of the host liquid type on the viscosity of gas-containing fluid samples.

Fig. 11 demonstrates that the viscosity of the water-based sample increased significantly when nitrogen was dissolved, followed by

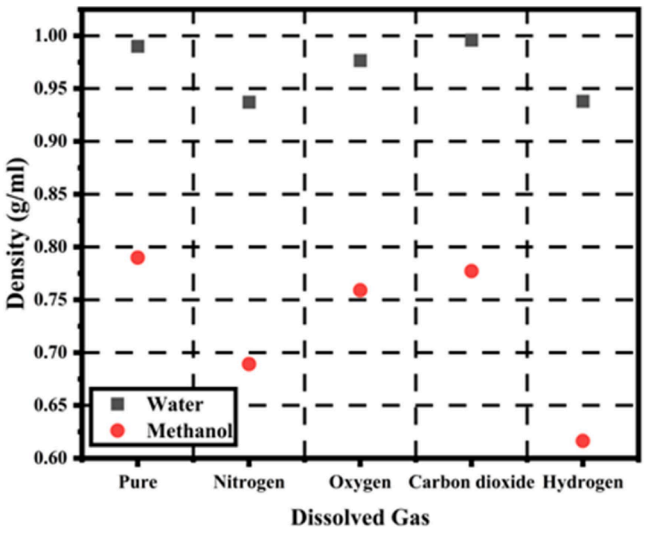

Fig. 9. Density of prepared samples with various gases.

oxygen and then carbon dioxide. The addition of hydrogen resulted in the smallest increase in viscosity. For the same weight fraction of dissolved gases, including nitrogen, oxygen, and carbon dioxide, it was observed that nitrogen and oxygen could form NBs within the water host medium. It was observed that, Fig. 6, the density of these formed NBs was significantly higher than that of the gas in the gas phase and near the liquid phase. Consequently, these NBs acted as obstacles, hindering molecular movement and thereby increasing resistance to motion, which in turn increased viscosity. As depicted in Fig. 6, the radius of the nitrogen-formed NB (40.36 Å) was larger than that of the oxygen-formed NBs (35.28 Å), further impacting the freedom of movement and resulting in the nitrogen nanobubble-containing water sample exhibiting higher viscosity than the oxygen-containing one. However, it's worth noting that while hydrogen could form NB in water with sizes similar to those of the formed oxygen NB, the viscosity of the hydrogen nanobubble-containing sample was lower than that of the non-nanobubbled carbon dioxide water sample. As shown in Fig. 6, the density of hydrogen NB is significantly less than that of oxygen NB. Upon delving deeper into the intermolecular forces between water and dissolved carbon dioxide and hydrogen, as depicted in Fig. 12, it becomes evident that the interaction strength between carbon dioxide molecules and water surpasses that between hydrogen molecules and water. This difference in interaction strength significantly affects the motion of host fluid molecules, ultimately resulting in the carbon dioxide-containing sample having higher viscosity than the hydrogen-containing one. This emphasizes that NBs with higher density may impede fluid flow more significantly than those with lower density, while in samples with lower-density NBs, molecular interactions assume a crucial role.

As Fig. 11 illustrates, among methanol samples, the most significant reduction in viscosity was observed in the hydrogen and nitrogen samples, followed by the oxygen sample, while the addition of carbon dioxide resulted in the smallest decrease in methanol-based viscosity. Notably, nitrogen was found to form NBs within the methanol host liquid. However, when comparing the density of these formed NBs in

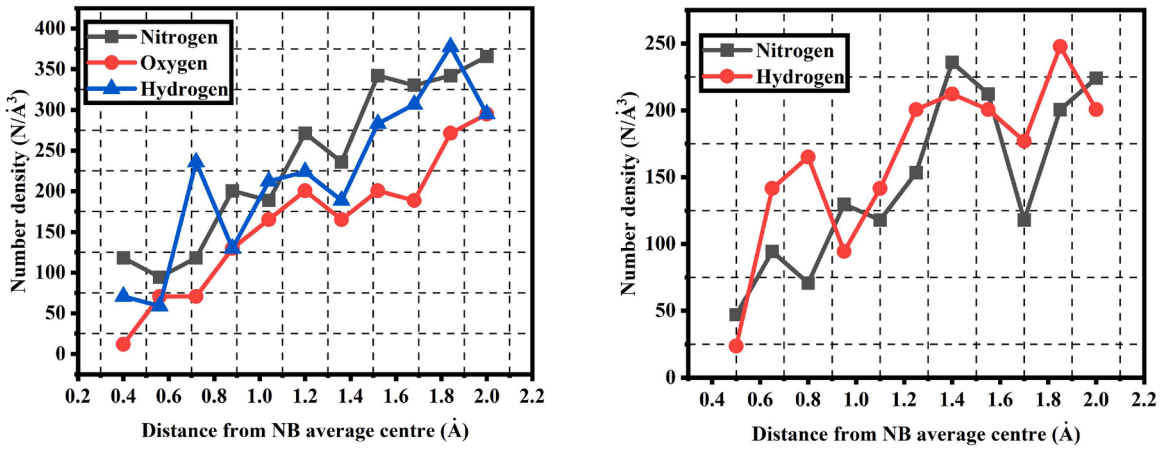

Fig. 10. Number densities of the host liquid molecules around the formed NB in (left) water and (right) methanol samples.

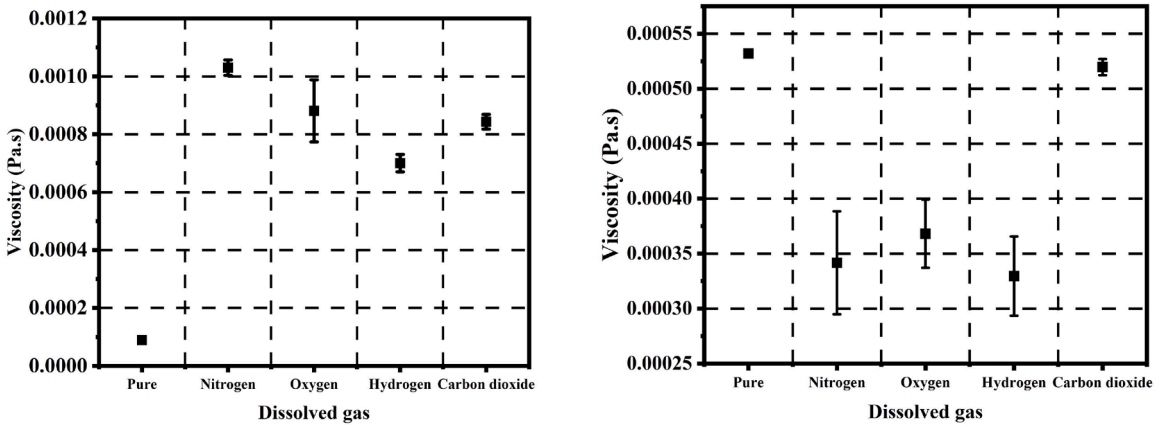

Fig. 11. The viscosity of samples containing dissolved gases in water (left) and methanol (right).

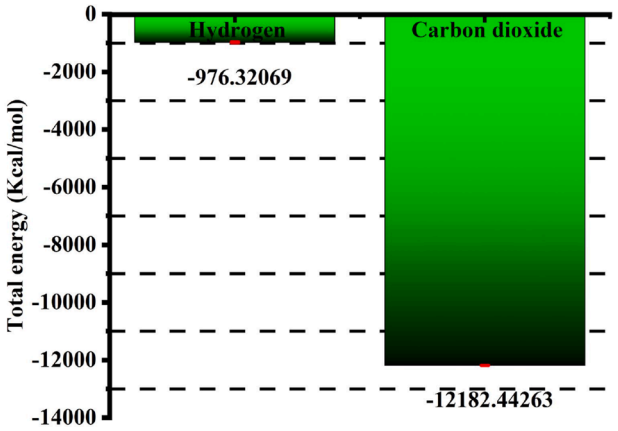

Fig. 12. The average of total energy between carbon dioxide and hydrogen molecules with water molecules.

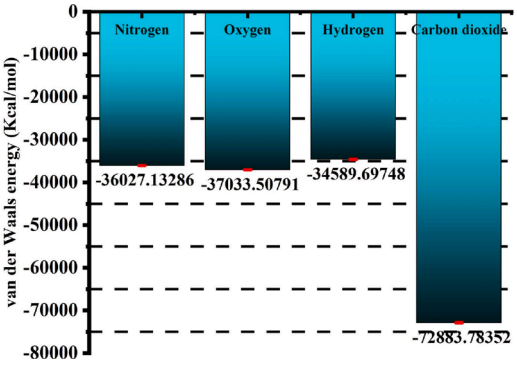

Fig. 13. The average of van der Waals energy of methanol mixtures.

methanol (0.125 g/ml) as shown in Table 2, it was lower than that of the formed nitrogen NBs (0.354 g/ml) in water as shown in Fig. 6. This indicates that molecular interactions play a dominant role in governing the viscosity of methanol-based samples. Fig. 13 provides insights into the van der Waals energy of methanol mixtures, emphasizing substantial variations in intermolecular forces. Precisely, the data demonstrates that the attractive forces within the carbon dioxide mixture are significantly more potent, leading to a heightened attraction that constrains the movement of atoms in this sample. Consequently, this intensified attraction results in higher viscosity compared to the other samples.

As depicted in Fig. 8, there is a notable correlation between temperature and intermolecular forces, and this relationship has a significant impact on the viscosity of the samples. At343.15 K, the viscosity of the nitrogen-water mixture was measured at 0.00053 Pa.s, while the nitrogen-methanol mixture at 323.15 K exhibited a viscosity of 0.00017 Pa.s. These findings indicate a decrease in viscosity compared to the viscosity of nitrogen samples at 298.15 K, as illustrated in Fig. 11. Additionally, with the increase in temperature, the kinetic energy of fluid molecules intensifies, causing them to move more rapidly and disperse. Consequently, this dispersion leads to a decrease in density. At elevated temperatures, the density measurements for nitrogen samples in water and methanol were recorded as 0.81 and 0.63 g/ml, respectively.

Conclusion

In this study, a combined approach involving molecular dynamics simulations and unsupervised machine learning was employed to investigate the nucleation and intrinsic properties of nanobubbles (NBs) within water and methanol liquids. Atomic-level insight was also utilized to explore the influence of NBs on the thermophysical properties of the host liquids. The results reveal that the nucleation of NBs depends on the interaction between solvent molecules, and the electron structure of the dissolved gas. The interaction between dispersed gases and host mediums is affected by the competition of solvent molecules for available intermolecular interaction sites. As a result, dissolved gases exhibit different behaviours in different solvents, as reflected by the observations that oxygen can form NB in polar host but cannot form any NBs in methanol. Moreover, the density of nitrogen NB formed differs between water and methanol, with observed values of 0.354 g/ml in water and 0.125 g/ml in methanol. In more viscous medium, the trapped gas molecules prefer to make stronger interactions, resulting in compact and denser NBs. The size and density of NBs also play a crucial role in their longevity in the host medium. As the size of NBs decreases, their density increases, leading to a higher surface area-to-volume ratio compared to larger gas bubbles. This results in stronger intermolecular forces between the gas and liquid phases, allowing gas atoms to be absorbed by the NB and increase its size which helps NB to survive in the host medium. The smallest NB can deform during a coalescence process due to the presence of London dispersion forces, which can facilitate the formation of a bridge-like shape. Moreover, the presence of these formed NBs has an impact on the density of the surrounding liquid. In water, the dissolution of nitrogen and hydrogen led to reductions of 6.4% and 5.91%, respectively, and in the methanol-based sample, the most substantial density decrease occurred during hydrogen dissolution, reaching 22.22%, attributed to the nanolayer formed around the NBs disrupting liquid molecule interactions. Notably, the viscosity of the host liquid is influenced by the presence of high-density NBs, as evidenced by the highest viscosities observed in nitrogen and oxygen nanobubbled water samples at 0.0013 and 0.00088 Pa.s, respectively. In contrast, non-nanobubbled samples or those with low-density NBs are primarily governed by molecular interactions, resulting in the smallest reduction observed in the methanol-based sample for non-bubbled carbon dioxide at 0.00052 Pa·s. It was also found that at elevated temperatures, nucleation is initiated by a smaller number of nucleation sites with a higher concentration of gas atoms.

CRediT authorship contribution statement

Hamidreza Hassanloo: Writing – review & editing, Writing – original draft, Visualization, Software, Methodology, Investigation, Formal analysis, Data curation, Conceptualization. **Xinyan Wang:** Writing – review & editing, Supervision, Resources, Project administration.

Declaration of competing interest

There is no conflict of interest to declare.

Data availability

the data of this paper can be accessed from the Brunel University London data archive, figshare at https://brunel.figshare.com

Acknowledgement

This work was supported by a UKRI Future Leaders Fellowship (MR/T042915/1) and EPSRC DTP (EP/T518116/1-2688449). MD simulations were run on ARCHER2 and MMM Hub Young, the UK's National Supercomputing Service, the data of this paper can be accessed from the Brunel University London data archive, figshare at https://brunel.figshare.com.

Supplementary materials

Supplementary material associated with this article can be found, in the online version, at doi:10.1016/j.ijft.2024.100734.

Reference

[1] E. Fabre, S.S. Murshed, A comprehensive review of thermophysical properties and prospects of ionanocolloids in thermal energy applications, Renewable and Sustainable Energy Reviews 151 (2021) 111593.
[2] I. Mahbubul, Preparation, characterization, properties, and application of nanofluid, William Andrew, 2018.
[3] M. Awais, A.A. Bhuiyan, S. Salehin, M.M. Ehsan, B. Khan, M.H. Rahman, Synthesis, heat transport mechanisms and thermophysical properties of nanofluids: A critical overview, International Journal of Thermofluids 10 (2021) 100086.
[4] Z. Said, et al., Recent advances on the fundamental physical phenomena behind stability, dynamic motion, thermophysical properties, heat transport, applications, and challenges of nanofluids, Physics Reports 946 (2022) 1–94.
[5] W. Wu, et al., Diffusivities in 1-alcohols containing dissolved H_2, He, N_2, CO, or CO_2 close to infinite dilution, The Journal of Physical Chemistry B 123 (41) (2019) 8777–8790.
[6] A. Kumagai, Y. Kawase, C. Yokoyama, Falling capillary tube viscometer suitable for liquids at high pressure, Review of scientific instruments 69 (3) (1998) 1441–1445.
[7] G. Graziano, Forever blowing nanobubbles, Nature Reviews Chemistry 4 (10) (2020) 506. -506.
[8] K. Phan, T. Truong, Y. Wang, B. Bhandari, Effect of CO_2 nanobubbles incorporation on the viscosity reduction of fruit juice concentrate and vegetable oil, International Journal of Food Science & Technology 56 (9) (2021) 4278–4286.
[9] H. Hu, et al., Quasi/non-equilibrium state in nanobubble growth trajectory revealed by in-situ transmission electron microscopy, Nano Today 48 (2023) 101761.
[10] M. Alheshibri, J. Qian, M. Jehannin, V.S. Craig, A history of nanobubbles, Langmuir 32 (43) (2016) 11086–11100.
[11] S.R. German, M.A. Edwards, H. Ren, H.S. White, Critical nuclei size, rate, and activation energy of H2 gas nucleation, Journal of the American Chemical Society 140 (11) (2018) 4047–4053.
[12] A.J. Atkinson, O.G. Apul, O. Schneider, S. Garcia-Segura, P. Westerhoff, Nanobubble technologies offer opportunities to improve water treatment, Accounts of chemical research 52 (5) (2019) 1196–1205.
[13] M.U. Farid, et al., Hybrid nanobubble-forward osmosis system for aquaculture wastewater treatment and reuse, Chemical Engineering Journal 435 (2022) 135164.
[14] K. Ebina, et al., Oxygen and air nanobubble water solution promote the growth of plants, fishes, and mice, PLoS One 8 (6) (2013) e65339.
[15] J. Zhu, et al., Cleaning with bulk nanobubbles, Langmuir 32 (43) (2016) 11203–11211.
[16] R. Chandan, R. Banerjee, Pro-apoptotic liposomes-nanobubble conjugate synergistic with paclitaxel: a platform for ultrasound responsive image-guided drug delivery, Scientific reports 8 (1) (2018) 1–15.
[17] X. Li, B. Peng, Q. Liu, J. Liu, L. Shang, Micro and nanobubbles technologies as a new horizon for CO_2-EOR and CO_2 geological storage techniques: A review, Fuel 341 (2023) 127661.
[18] S.H. Oh, S.H. Yoon, H. Song, J.G. Han, J.-M. Kim, Effect of hydrogen nanobubble addition on combustion characteristics of gasoline engine, International journal of hydrogen energy 38 (34) (2013) 14849–14853.
[19] L. Zhou, S. Wang, L. Zhang, J. Hu, Generation and stability of bulk nanobubbles: A review and perspective, Current Opinion in Colloid & Interface Science 53 (2021) 101439.
[20] F. Eklund, M. Alheshibri, J. Swenson, Differentiating bulk nanobubbles from nanodroplets and nanoparticles, Current Opinion in Colloid & Interface Science 53 (2021) 101427.
[21] M. Alheshibri, V.S. Craig, Generation of nanoparticles upon mixing ethanol and water; Nanobubbles or Not? Journal of colloid and interface science 542 (2019) 136–143.
[22] A. Häbich, W. Ducker, D.E. Dunstan, X. Zhang, Do stable nanobubbles exist in mixtures of organic solvents and water? The Journal of Physical Chemistry B 114 (20) (2010) 6962–6967.
[23] L. Sun, et al., Research progress on bulk nanobubbles, Particuology 60 (2022) 99–106.
[24] P.S. Epstein, M.S. Plesset, On the stability of gas bubbles in liquid-gas solutions, The Journal of Chemical Physics 18 (11) (1950) 1505–1509.
[25] E.D. Michailidi, et al., Bulk nanobubbles: Production and investigation of their formation/stability mechanism, Journal of colloid and interface science 564 (2020) 371–380.
[26] B.H. Tan, H. An, C.-D. Ohl, How bulk nanobubbles might survive, Physical review letters 124 (13) (2020) 134503.
[27] B.H. Tan, H. An, C.-D. Ohl, Stability of surface and bulk nanobubbles, Current Opinion in Colloid & Interface Science 53 (2021) 101428.
[28] D. Lohse, X. Zhang, Pinning and gas oversaturation imply stable single surface nanobubbles, Physical Review E 91 (3) (2015) 031003.
[29] K. Ohgaki, N.Q. Khanh, Y. Joden, A. Tsuji, T. Nakagawa, Physicochemical approach to nanobubble solutions, Chemical Engineering Science 65 (3) (2010) 1296–1300.
[30] J.H. Weijs, J.R. Seddon, D. Lohse, Diffusive shielding stabilizes bulk nanobubble clusters, ChemPhysChem 13 (8) (2012) 2197–2204.
[31] S.A. Bagherzadeh, S. Alavi, J. Ripmeester, P. Englezos, Formation of methane nano-bubbles during hydrate decomposition and their effect on hydrate growth, The Journal of chemical physics 142 (21) (2015) 214701.
[32] S.-Y. Liu, et al., Quasi-2D liquid cell for high density hydrogen storage, Nano Energy 31 (2017) 218–224.
[33] B. Bhushan, Y. Wang, A. Maali, Coalescence and movement of nanobubbles studied with tapping mode AFM and tip–bubble interaction analysis, Journal of Physics: Condensed Matter 20 (48) (2008) 485004.
[34] T. Koishi, et al., Nanoscale hydrophobic interaction and nanobubble nucleation, Physical review letters 93 (18) (2004) 185701.
[35] M. Zhang, Y.-s. Tu, H.-p. Fang, Concentration of nitrogen molecules needed by nitrogen nanobubbles existing in bulk water, Applied Mathematics and Mechanics 34 (12) (2013) 1433–1438.
[36] Z. Gao, W. Wu, W. Sun, B. Wang, Understanding the stabilization of a bulk nanobubble: A molecular dynamics analysis, Langmuir 37 (38) (2021) 11281–11291.
[37] Y. Lu, L. Yang, Y. Kuang, Y. Song, J. Zhao, A.K. Sum, Molecular simulations on the stability and dynamics of bulk nanobubbles in aqueous environments, Physical Chemistry Chemical Physics 23 (48) (2021) 27533–27542.
[38] S.A. Hewage, J.N. Meegoda, Molecular dynamics simulation of bulk nanobubbles, Colloids and Surfaces A: Physicochemical and Engineering Aspects 650 (2022) 129565.
[39] E. Bird, E. Smith, Z. Liang, Coalescence characteristics of bulk nanobubbles in water: A molecular dynamics study coupled with theoretical analysis, Physical Review Fluids 6 (9) (2021) 093604.
[40] E. Bird, J. Zhou, Z. Liang, Coalescence speed of two equal-sized nanobubbles, Physics of Fluids 32 (12) (2020).
[41] W. Wang, et al., Solid–liquid–gas reaction accelerated by gas molecule tunnelling-like effect, Nature Materials 21 (8) (2022) 859–863.
[42] A. Angulo, P. van der Linde, H. Gardeniers, M. Modestino, D.F. Rivas, Influence of bubbles on the energy conversion efficiency of electrochemical reactors, Joule 4 (3) (2020) 555–579.
[43] A. Glielmo, B.E. Husic, A. Rodriguez, C. Clementi, F. Noé, A. Laio, Unsupervised learning methods for molecular simulation data, Chemical Reviews 121 (16) (2021) 9722–9758.
[44] C. Bie, L. Wang, J. Yu, Challenges for photocatalytic overall water splitting, Chem 8 (6) (2022) 1567–1574.
[45] F.D. Tovar, M.A. Barrufet, D.S. Schechter, Enhanced oil recovery in the wolfcamp shale by carbon dioxide or nitrogen injection: An experimental investigation, SPE Journal 26 (01) (2021) 515–537.
[46] L. Qiu, et al., A review of recent advances in thermophysical properties at the nanoscale: From solid state to colloids, Physics Reports 843 (2020) 1–81.
[47] P. Bayer, L. Rybach, P. Blum, R. Brauchler, Review on life cycle environmental effects of geothermal power generation, Renewable and Sustainable Energy Reviews 26 (2013) 446–463.
[48] F. Schorn, et al., Methanol as a renewable energy carrier: An assessment of production and transportation costs for selected global locations, Advances in Applied Energy 3 (2021) 100050.
[49] M.A. Ghadikolaei, C.S. Cheung, K.-F. Yung, Study of combustion, performance and emissions of a diesel engine fueled with ternary fuel in blended and fumigation modes, Fuel 235 (2019) 288–300.
[50] E.O. Pyzer-Knapp, et al., Accelerating materials discovery using artificial intelligence, high performance computing and robotics, npj Computational Materials 8 (1) (2022) 84.
[51] S. Bayda, M. Adeel, T. Tuccinardi, M. Cordani, F. Rizzolio, The history of nanoscience and nanotechnology: from chemical–physical applications to nanomedicine, Molecules 25 (1) (2019) 112.
[52] H. Hassanloo, S. Sadeghzadeh, R. Ahmadi, A new approach to dispersing and stabilizing graphene in aqueous nanofluids of enhanced efficiency of energy-systems, Scientific Reports 10 (1) (2020) 1–11.
[53] M.P. Allen, Introduction to molecular dynamics simulation, Computational soft matter: from synthetic polymers to proteins 23 (1) (2004) 1–28.
[54] W.L. Jorgensen, D.S. Maxwell, J. Tirado-Rives, Development and testing of the OPLS all-atom force field on conformational energetics and properties of organic liquids, Journal of the American Chemical Society 118 (45) (1996) 11225–11236.
[55] Q. Yang, C. Zhong, Molecular simulation of adsorption and diffusion of hydrogen in metal– organic frameworks, The Journal of Physical Chemistry B 109 (24) (2005) 11862–11864.
[56] K. Chae, A. Violi, Mutual diffusion coefficients of heptane isomers in nitrogen: A molecular dynamics study, The Journal of chemical physics 134 (4) (2011) 044537.
[57] C. Sun, B. Wen, B. Bai, Application of nanoporous graphene membranes in natural gas processing: Molecular simulations of CH4/CO2, CH4/H2S and CH4/N2 separation, Chemical engineering science 138 (2015) 616–621.
[58] S. Jain, L. Qiao, Molecular dynamics simulations of the surface tension of oxygen-supersaturated water, AIP Advances 7 (4) (2017) 045001.
[59] J.L. Abascal, C. Vega, A general purpose model for the condensed phases of water: TIP4P/2005, The Journal of chemical physics 123 (23) (2005) 234505.
[60] S. Plimpton, Fast parallel algorithms for short-range molecular dynamics, Journal of computational physics 117 (1) (1995) 1–19.
[61] A. Stukowski, Visualization and analysis of atomistic simulation data with OVITO–the Open Visualization Tool, Modelling and simulation in materials science and engineering 18 (1) (2009) 015012.

[62] K.R. Harris, L.A. Woolf, Pressure and temperature dependence of the self diffusion coefficient of water and oxygen-18 water, Journal of the Chemical Society, Faraday Transactions 1: Physical Chemistry in Condensed Phases 76 (1980) 377–385.
[63] W.S. Price, H. Ide, Y. Arata, Solution dynamics in aqueous monohydric alcohol systems, The Journal of Physical Chemistry A 107 (24) (2003) 4784–4789.
[64] M. Ester, H.-P. Kriegel, J. Sander, X. Xu, A density-based algorithm for discovering clusters in large spatial databases with noise, kdd 96 (34) (1996) 226–231.
[65] K. Dill, S. Bromberg, Molecular driving forces: statistical thermodynamics in biology, chemistry, physics, and nanoscience, Garland Science, 2010.
[66] L. Gevantman, Solubility of selected gases in water, Nitric oxide (NO) 308 (3.348) (2000) 10–14.
[67] S. Alavi, Molecular simulations: fundamentals and practice, John Wiley & Sons, 2020.
[68] J.I. Lee, H.S. Huh, J.Y. Park, J.-G. Han, J.-M. Kim, Coarsening behavior of bulk nanobubbles in water, Scientific Reports 11 (1) (2021) 19173.
[69] M. Kerscher, et al., Thermophysical properties of the energy carrier methanol under the influence of dissolved hydrogen, International Journal of Hydrogen Energy (2023).